AUTOMATIC APPROACH FOR CALIBRATING OFF-THE-SHELF DIGITAL CAMERAS

A. F. Habib[a], M. F. Morgan[a]

[a] Department of Geomatics Engineering, University of Calgary
2500 University Drive NW, Calgary AB T2N 1N4, Canada - (habib, morgan)@geomatics.ucalgary.ca

Commission I, WG I/6

KEY WORDS: Straight line, Self-Calibration, Bundle Adjustment and Digital Cameras

ABSTRACT:

Recent developments of digital cameras in terms of size of Charged Coupled Device (CCD) arrays and reduced costs are leading to their applications to traditional as well as new photogrammetric, surveying, and mapping functions. Digital cameras, intended to replace the conventional film based mapping cameras, are becoming available along with many smaller format digital cameras capable of precise measurement applications. All such cameras require careful assessment to determine their metric characteristics, which are essential to carry out photogrammetric activities. These characteristics include estimates of the calibrated focal length, location of the principal point relative to the array coordinate system, lens distortion, and the short and long-term stability of these quantities. These characteristics are known collectively as the Interior Orientation Parameters (IOP). Current calibration methods are based on traditional test fields with numerous distinct targets, which have to be professionally surveyed prior to the calibration procedure in order to precisely determine their three-dimensional coordinates. Establishing, surveying, and maintaining traditional calibration test fields are very expensive and not easy tasks for non-photogrammetric users of digital cameras. This paper relates to the development of a new laboratory calibration procedure that requires an easy-to-establish calibration test field (group of straight lines). In addition, the whole calibration process can be automatically carried out with minimal human interaction. It is expected that this calibration procedure would provide a good tool for studying the short and long-term stability of off-the-shelf digital cameras. In addition, it will give a great push to using those cameras in large scale mapping applications as well as various close range photogrammetric activities.

1. INTRODUCTION

Recently, there has been a growing interest in utilizing linear features instead of distinct points in various photogrammetric operations. Linear features are easier to extract than distinct points, especially in a digital environment (Kubik, 1991), and they can be extracted with sub-pixel accuracy. Moreover, linear features possess more semantic information, when compared to distinct points, regarding the object space as they in most of the cases represent object boundaries. As far as the camera calibration is concerned, it is much easier to establish a test field comprised of straight lines rather than establishing a traditional test field with numerous ground control points.

Traditional analytical camera calibration through bundle adjustment requires a test field with numerous control points that have to be precisely surveyed prior to the calibration process. Establishing and maintaining such a test field is an expensive procedure that has to be conducted by professionals. Brown (1971) introduced plumb-line method that uses straight lines to derive radial and decentric lens distortions. The principle behind this method is that straight line in object space should project through a perfect lens as straight-line image. Any variations from straightness in the image space are attributed to radial and decentric distortions. This method offers a rapid and practical procedure for computing lens distortion parameters. However, the results would be contaminated by uncorrected systematic errors in the comparator and uncompensated film deformations. Moreover, we still need to perform a separate calibration procedure for determining the camera constant and other systematic distortions such as affine deformations. Heuvel

(1999b) proposed another approach for using straight lines to recover the Interior Orientation Parameters (IOP). This method can only be applied whenever we have imagery containing parallel and perpendicular lines. Similar to the plumb-line method, the radial lens distortion is estimated first. Then, the principal point coordinates and the focal length are determined later.

Prior to incorporating straight lines in the bundle adjustment procedure, a decision should be made regarding how they would be represented in image and object space. Within most of the existing literature such as the work of Mulawa and Mikhail (1988), Tommaselli and Lugnani (1988), Ayache and Faugeras (1989), Tommaselli and Tozzi (1992), Habib (1998), Heuvel (1999a) and Tommaselli and Poz (1999), a straight line in the object space is defined as an infinite line using minimal representation with four degrees of freedom. Habib (1999) proposed an alternative approach for representing object space straight lines using two points (six-dimensional representation). Uniqueness and singularies are the primary reasons for choosing this representation. Since minimal representations of object space line as an infinite one have singularities, they would not represent all three-dimensional lines in object space. In addition, such a representation would require complicated algorithms for perspective transformation between object and image space, which would make it difficult to incorporate in existing bundle adjustment programs. In this research, we use two points to represent the straight lines in object space, as suggested by Habib (1999). Thus, the object space line segments would be well localized. On the other hand, image space lines will be represented as a sequence of 2-D points.

This representation would allow us to incorporate various distortions at each point along the line.

This paper introduces a new approach for simultaneous estimation of the IOP of cameras. This method can utilize straight lines as well as distinct points in the bundle adjustment with self-calibration. Section 2 summarizes commonly used distortion models and traditional analytical camera calibration procedure. The suggested mathematical model for incorporating straight lines in bundle adjustment with self-calibration is described in section 3. Then, we present experimental results obtained from the suggested approach using real data. Finally, conclusions and recommendations for future work are summarized in section 5.

2. SELF-CALIBRATION: BACKGROUND

The main objective of photogrammetry is to inverse the process of photography. When the film or CCD array inside the camera is exposed to light, light rays from the object space pass through the camera perspective centre (the lens) until they hit the focal plane (film or CCD array) producing images of the photographed objects. Light rays from the object points to the corresponding image points passing through the lens are assumed to be straight. This assumption is known in the photogrammetric literature as the collinearity model (Kraus, 1993).

During camera calibration, we determine the IOP, which comprise the coordinates of the principal point, the principal distance, and image coordinate corrections that compensate for various deviations from the collinearity model. There are four principal sources of departure from collinearity, which are "physical" in nature (Fraser, 1997). These are the radial lens distortion, decentric lens distortion, image plane unflatness, and in plane image distortion. The net image displacement at any point is the cumulative influence of these perturbations. The relative magnitude of each one of these perturbations depends very much on the quality of the camera being employed.

2.1 Distortion models

Radial lens distortion is usually represented by polynomial series (Equation 1). The term K_1 alone will usually suffice in medium accuracy applications. The inclusion of K_2 and K_3 terms might be required for higher accuracy and wide-angle lenses. The decision as to whether to incorporate one, two or three radial distortion terms can be based on statistical tests of significance.

$$\Delta x_{RLD} = K_1(r^2-1)x + K_2(r^4-1)x + K_3(r^6-1)x$$
$$\Delta y_{RLD} = K_1(r^2-1)y + K_2(r^4-1)y + K_3(r^6-1)y \qquad (1)$$

where

$$r = \sqrt{(x-x_p)^2 + (y-y_p)^2}$$

and K_1, K_2 and K_3 are the radial lens distortion parameters.

A lack of centring of the lens elements along the optical axis gives rise to the second category of lens distortion, namely, decentric distortion. The misalignment of the lens components cause both radial and tangential distortions which can be modelled by correction equations according to (Brown, 1966) as follows:

$$\Delta x_{DLD} = P_1(r^2+2x^2) + 2P_2xy$$
$$\Delta y_{DLD} = P_2(r^2+2y^2) + 2P_1xy \qquad (2)$$

where P_1 and P_2 are the decentric lens distortion parameters.

Systematic image coordinate errors due to focal plane unflatness can limit the accuracy of photogrammetric triangulation. Radial image displacement induced by focal plane unflatness depends on the incidence angle of the imaging ray. Narrow angle lenses of long focal length are much less influenced by out-of-plane image deformation than short focal length and wide-angle lenses. To compensate for focal plane unflatness, the focal plane needs to be topographically measured. Then, a third- or fourth-order polynomial can model the resulting image coordinate perturbations. In this work, the effect of focal plane unflatness is assumed to be very small and will be ignored.

In-plane distortions are usually manifested in differential scaling between x and y image coordinates. In addition, in-plane distortions might introduce image axes non-orthogonality. Those distortions are usually denoted affine deformations and can be mathematically described by Equation 3. One should note that affine deformation parameters, which are correlated with other IOP and EOP are eliminated (for example, shifts are eliminated since they are correlated with the principal point coordinates).

$$\Delta x_{AD} = -A_1x + A_2y$$
$$\Delta y_{AD} = A_1y \qquad (3)$$

where A_1 and A_2 are the affine distortion parameters.

2.2 Traditional approach of camera calibration

In traditional camera calibration, convergent imagery is acquired over a test field. Together with tie points, a large number of control points are measured in both image and object space. The extended collinearity equations (Equations 4 and 5) are used in bundle adjustment with self-calibration to solve for:
- Ground coordinates of tie points.
- EOP of the involved imagery.
- IOP of the involved camera(s).

$$x_a = x_p - c\frac{r_{11}(X_A-X_0)+r_{21}(Y_A-Y_0)+r_{31}(Z_A-Z_0)}{r_{13}(X_A-X_0)+r_{23}(Y_A-Y_0)+r_{33}(Z_A-Z_0)} + \Delta x \quad (4)$$

$$y_a = y_p - c\frac{r_{12}(X_A-X_0)+r_{22}(Y_A-Y_0)+r_{32}(Z_A-Z_0)}{r_{13}(X_A-X_0)+r_{23}(Y_A-Y_0)+r_{33}(Z_A-Z_0)} + \Delta y \quad (5)$$

where:
$\Delta x = \Delta x_{RLD} + \Delta x_{DLD} + \Delta x_{AD} + \Delta x_{etc}$,
$\Delta y = \Delta y_{RLD} + \Delta y_{DLD} + \Delta y_{AD} + \Delta y_{etc}$,

(x_a, y_a) — are the observed image coordinates of image point a,
(X_A, Y_A, Z_A) — are the ground coordinates of object point A,
(x_p, y_p) — are the image coordinates of the principal point,
c — is the camera constant (principal distance),
(X_0, Y_0, Z_0) — are the ground coordinates of the perspective centre, and
$(r_{11}, …, r_{33})$ — are the elements of the rotation matrix that depend on the rotation angles (ω, φ, κ).

3. SUGGESTED APPROACH

3.1 Mathematical Model

Before discussing the mathematical model, it should be noted that we want to incorporate overlapping images with straight linear features, some tie and control points in a self-calibration process to estimate the following parameters:

- The EOP of the involved imagery and the IOP of the involved cameras.
- The ground coordinates of tie points and the parameters defining the straight lines in the object space.

As shown in Figure 1, for a frame camera, a straight line in the object space will be a straight line in the image space in the absence of distortions. Deviation from straightness in the image space is a function of the distortion parameters. As mentioned before, including straight lines in the bundle adjustment procedure would require the answer to two main questions. First, what is the most convenient model for representing straight lines in the object and image space? Second, how can we establish the perspective relationship between image and object space lines? In this research, two points along the line represent object space line. Those points are monoscopically measured in one or two images within which this line appears. The relationship between those points and the corresponding object space points is modelled by the collinearity equations (Equations 4 and 5). In the image space, the lines will be defined by a sequence of intermediate points along the line. Once again, those points are monoscopically measured (there is no need to identify conjugate points in overlapping images). This representation is useful since it allows us to individually model and include the distortions at each of these points. The perspective relationship between image and object space lines is incorporated in a mathematical constraint. The underlying principle in this constraint is that the vector from the perspective centre to any intermediate image point along the line lies on the plane defined by the perspective centre of that image and the two points defining the straight line in the object space. In other words, the three vectors (Figures 1 and 2):

- $\mathbf{v}_1$ (the vector connecting the perspective centre to the first point along the object space line).
- $\mathbf{v}_2$ (the vector connecting the perspective centre to the second point along the object space line).
- $\mathbf{v}_3$ (the vector connecting the perspective centre to any intermediate point along the image line) are coplanar (Equation 6).

$$(\mathbf{v}_1 \times \mathbf{v}_2) \circ \mathbf{v}_3 = 0 \qquad (6)$$

Equation 6 incorporates the image coordinates of the intermediate point, EOP, IOP (which includes the distortion parameters) as well as the ground coordinates of the points defining the object space line. The constraint in Equation 6 can be written for each intermediate point along the line in the imagery. One should note that this constraint would not introduce any new parameters. The number of constraints is equal to the number of measured intermediate points along the image line.
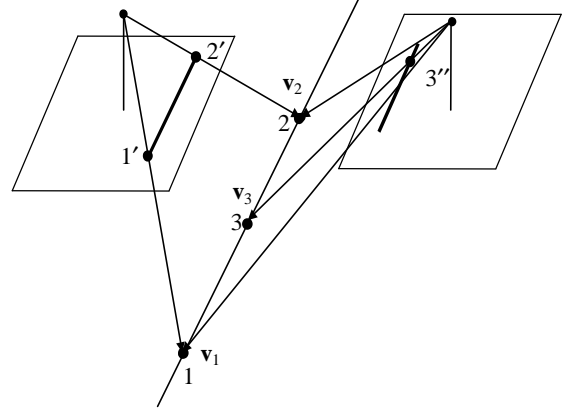
Figure 1. 3-D straight lines in frame camera imagery.

$$\mathbf{v}_3 = \mathbf{R}(\omega,\varphi,\kappa) \begin{bmatrix} x - x_p - \text{distortion}_x \\ y - y_p - \text{distortion}_y \\ -c \end{bmatrix}$$
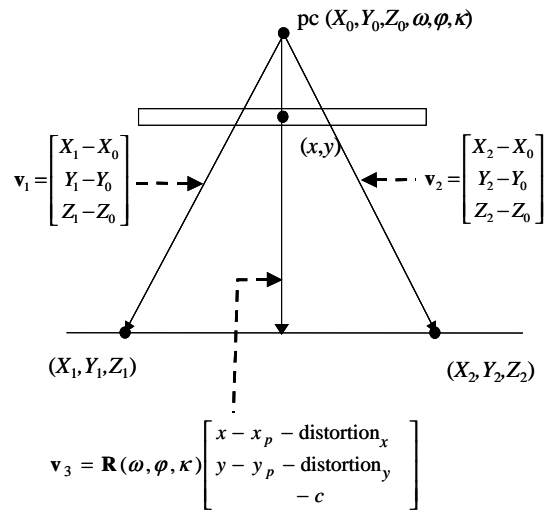
Figure 2. Mathematical model for including straight lines in frame camera imagery.

In summary, for bundle adjustment with self-calibration using straight lines, the end points (points 1 and 2 in the above example) can be selected in any of the images where the straight line appears. These points need not be identifiable or even visible in other images. Four collinearity equations will be written using the measured end points for each line. The intermediate points (point 3 in the above example) can be measured in any one of the overlapping images. Those intermediate points need not be conjugate. A constraint is written for each intermediate point according to Equation 6. A schematic drawing to clarify the different scenarios for the end point selection is shown in Figure 3. Figure 3-a shows a case where the end points of the straight line are selected in one image (image 1); while in Figure 3-b, they are selected in different images (images 1 and 4). Intermediate points are shown in the same figure.

The same approach can be extended to include higher-order primitives (for example, conic sections). In addition, it is applicable for line cameras as well. The only difference is that the platform motion perturbations during the scene capture as well as the above mentioned distortion sources cause deviation from straightness in the imagery.
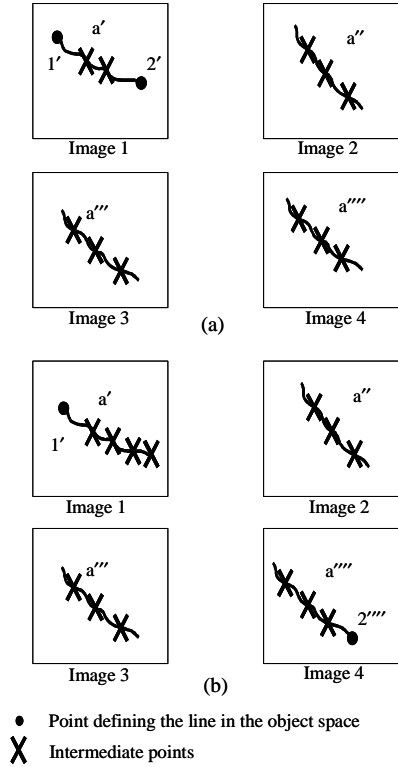
Figure 3. Schematic drawing representing two scenarios for the selection of the end and intermediate points in overlapping images.

3.2 Optimal configuration

Two types of configurations of straight lines, box-type (Figure 4) and X-type (Figure 5), are used to test the effects of previous distortion models. The optimum configuration is the one that will cause more deviations from straightness in the image space. Figures 4 and 5 illustrate the effects of various distortion sources for both configurations.
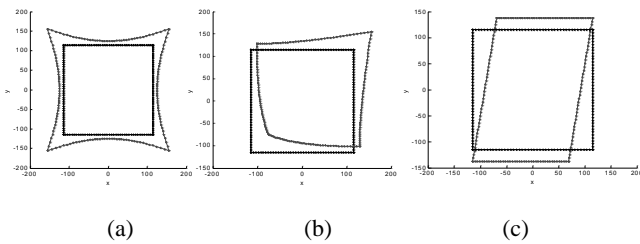
Figure 4. Distortions in box-type configuration: radial distortion (a), decentric distortion (b), and Affine deformation (c).
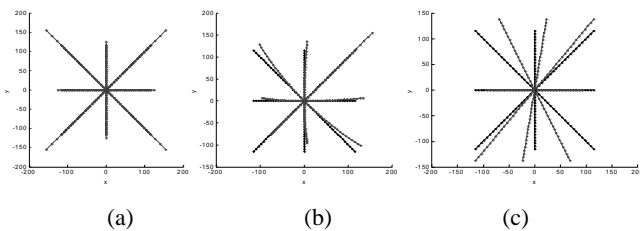
Figure 5. Distortions in X-type configuration: radial distortion (a), decentric distortion (b), and Affine deformation (c).

By analysing Figures 4 and 5, one can see that the box-type configuration is more useful since it causes larger deviation from straightness (compare Figure 4-a and 5-a). Therefore, to successfully recover the radial distortion parameters (the most significant distortion component), we need a test field composed of a grid of straight lines along the rows and columns of the captured calibration images. We also need some point targets to derive the camera constant (principal distance). These targets need not be surveyed with a theodolite or total station. Only distances between those targets should be measured. An example of such a test field can be seen in Figure 6.

4. EXPERIMENTAL RESULTS

Conducted experiments using real data are primarily focused on achieving the following objectives:
- Determine the required distortion parameters to sufficiently describe the IOP of the involved camera.
- Compare the performance of the suggested approach to the traditional approach using distinct ground control points.
- Inspect the accuracy of the reconstructed object space using the derived IOP.

In those experiments, we used a SONY DSC-F707 digital camera, with a maximum resolution of 2560 x 1920 pixels. A total of forty-eight images have been acquired in four different sessions (A-D). Using a shutter speed of 125, images used for experiment A and B were acquired with an f/number of 3.5. Then, an f/number of 11 is applied for experiments C and D. Each session consists of twelve exposures at six different locations with 90° rotation around the Z-axis at each exposure station. The camera was switched off/on after each session. We built a test field based on the optimal configuration discussed before, Figure 6. The test field is composed of nine straight lines (black robes on a white background). Also, distances between five targets (highlighted by black circles) have been measured (±2.0mm). We developed an automated procedure for measuring intermediate point coordinates along the lines in the involved imagery.
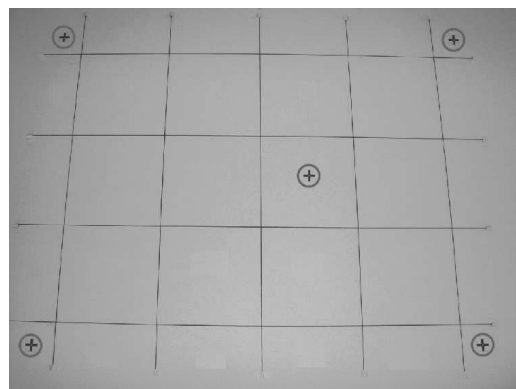
Figure 6. New test field

The test field has been augmented to allow for traditional point based camera calibration. A total of 30 signalised targets are precisely surveyed using a total station (±0.5mm), Figure 7-a. In the bundle adjustment with self-calibration, we can consider the following deformation/distortion parameters:
- Radial distortion parameters K_1, K_2.
- Decentric distortion parameters P_1, P_2.
- Affine deformation parameters A_1, A_2.

We carried out several experiments, using both point-based and line-based self-calibration, to investigate the most appropriate model that sufficiently describes the internal characteristics of the camera. Considering K_1, K_2, P_1, P_2, A_1, A_2 resulted in high correlations between parameters. In general, the following could be observed:

- There is high correlation between K_1 and K_2.
- There is high correlation between x_p and P_1.
- There is high correlation between y_p and P_2.
- There is high correlation between the IOP and EOP when using point-based self-calibration. This correlation is not observed when using line-based self-calibration.
- The estimated A_1 and A_2 are not significantly different from zero. This indicates that there are no affine deformations associated with the involved camera.

Moreover, using four parameters (x_p, y_p, c, K_1) resulted in a variance component (σ_0^2) that is not significantly different from the variance component obtained by considering nine IOP (x_p, y_p, c, K_1, K_2, P_1, P_2, A_1, A_2). Therefore, we concluded that considering x_p, y_p, c, K_1 sufficiently models the IOP of the involved camera.

Derived estimates of IOP using the traditional point-based and the developed line-based self-calibration procedures are shown in Table 1. Through visual inspection, results from both approaches are quite comparable. Also, by comparing results from Experiments A through D, we observe that the IOP of the involved camera has no significant variation between experiments. This indicates that the internal characteristics of the camera are stable over short time periods.

Table 1. Estimates of IOP and distortion parameter

Experiment A	Point	Line
σ_0	0.0018	0.0020
x_p [mm]	-0.1223 (±0.0046)	-0.1169 (±0.0016)
y_p [mm]	-0.0756 (0.0048)	-0.0648 (±0.0016)
c [mm]	11.6042 (±0.0124)	11.6094 (±0.0048)
K_1	-1.110829e-03	-1.176255e-03
Experiment B	**Point**	**Line**
σ_0	0.0018	0.0020
x_p [mm]	-0.1285 (±0.0042)	-0.1216 (±0.0016)
y_p [mm]	-0.0812 (±0.0043)	-0.0718 (±0.0015)
c [mm]	11.6101 (±0.0103)	11.6189 (±0.0044)
K_1	-1.10495e-03	-1.185481e-03
Experiment C	**Point**	**Line**
σ_0	0.0017	0.0019
x_p [mm]	-0.1247 (±0.0040)	-0.1224 (±0.0016)
y_p [mm]	-0.0707 (±0.0042)	-0.0642 (±0.0015)
c [mm]	11.6041 (±0.0118)	11.6034 (±0.0048)
K_1	-1.118769e-03	-1.174221e-03
Experiment D	**Point**	**Line**
σ_0	0.0018	0.0021
x_p [mm]	-0.1212 (±0.0044)	-0.1171 (±0.0016)
y_p [mm]	-0.0759 (±0.0044)	-0.0711 (±0.0016)
c [mm]	11.6090 (±0.0114)	11.6016 (±0.0047)
K_1	-1.121013e-03	-1.177155e-03

Intersections of conjugate light rays have been used to compare the IOP derived from the point-based and line-based calibration techniques (to see if there were significant differences between the estimated IOP). In those experiments, we used the following to compute object coordinates:

- IOP from point-based and line-based approaches to self-calibration.
- Image coordinate measurements of the signalised targets.
- One set of EOP

Reconstructed object spaces using the different IOP are compared through root mean square error analysis (Table 2). From the RMSE results in Table 2, one can see that the IOP from the point and line-based calibration procedures are stochastically identical.

Table 2. Intersection results (30 points)

RMSE	Exp. A	Exp. B	Exp. C	Exp. D
RMS_X [m]	0.00030	0.00036	0.00047	0.00073
RMS_Y [m]	0.00035	0.00025	0.00047	0.00065
RMS_Z [m]	0.00094	0.00078	0.00040	0.00073

In order to evaluate the quality of the derived IOP, the images have been re-sampled after removing various distortions (Figure 7-b). One can see that the straightness property has been correctly restored. A quantitative measure is developed using regression analysis applied to the measured intermediate points along the straight lines before and after calibration (namely, the variance component resulting from straight line fitting through the intermediate points). These results can be seen in Figure 7-b. The computed variance components after calibration are significantly improved after the calibration process.
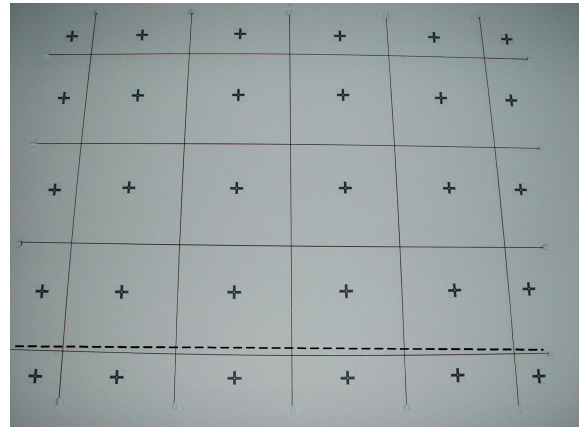
(a)
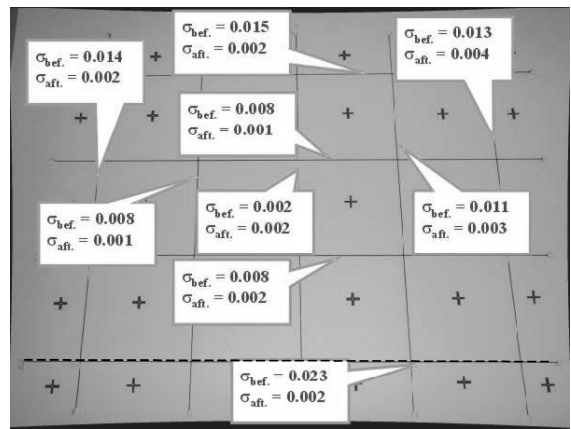
(b)

Figure 7. Original images before (a) and resampled images after (b) calibration. A dashed straight line has been added to show the deviation from straightness before calibration (a) and its recovery after calibration (b).

5. CONCLUSIONS AND REMARKS

In this research, straight line constraints are incorporated in bundle adjustment with self-calibration. Experiment results proved the feasibility of the suggested approach. The IOP derived from the suggested approach are stochastically identical to the derived IOP from the traditional point-based calibration procedure. It has been established that one radial distortion coefficient (K_1) is enough to model the distortions in the involved camera. The suggested approach has the following advantages:

- Compared to traditional point-based calibration test filed, the required test field is much easier to establish.
- Automation of the intermediate point measurements along the linear features improves the efficiency of the suggested approach.
- Non-photogrammetric users of off-the-shelf digital cameras can carry out the calibration procedure. This is important since it will allow such users to generate high quality photogrammetric products from digital cameras.
- For unstable digital cameras, the calibration procedure can be carried out every time the camera is switched on.
- The approach offers an effective tool to study the short-term and long-term stability of off-the-shelf digital camera and the most appropriate model that sufficiently describes various deformations taking place during the imaging process.

Future work will focus on more elaborate testing of the short and long-term stability of off-the-shelf digital cameras. We will investigate other distortion models to see if they can describe digital cameras more successfully. Finally, we will build a complete system that allows the user to perform three-dimensional measurements of the objects of interest (e.g. if those objects can be incorporated in the calibration test field, then the calibration and measurements can be done simultaneously).

REFERENCE

Ayache, N. and Faugeras, O., 1989. Maintaining representations of the environment of a mobile robot. *IEEE Transactions on Robotics Automation*, 5 (6): 804-819.

Brown, D. C., 1966. Decentric distortion of lenses. *Journal of Photogrammetric Engineering & Remote Sensing*, 32 (3): 444-462.

Brown, D. C., 1971. Close range camera calibration. *Journal of Photogrammetric Engineering & Remote Sensing*, 37 (8): 855-866.

Fraser, C., 1997. Digital self-calibration. *ISPRS Journal of Photogrammetry & Remote Sensing*, 52(1997): 149-159.

Habib, A., 1998. Motion parameter estimation by tracking stationary three-dimensional straight lines in image sequences. *ISPRS Journal of Photogrammetry & Remote Sensing*, 53 (1998): 174-182.

Habib, A., 1999. Aerial triangulation using point and linear features. *Proceedings of the ISPRS Conference on Automatic Extraction of GIS Objects from Digital Imagery*, Munich, Germany, 32 (3-2W5). 226 pages: 137-142.

Heuvel, F., 1999-a. A line-photogrammetric mathematical model for the reconstruction of polyhedral objects. *Videometrics VI, Proceedings of SPIE*, Vol. 3641: 60-71.

Heuvel, F. 1999-b. Estimation of interior orientation parameters from constraints on line measurements in a single image. *Proceedings of International Archives of Photogrammetry and Remote Sensing*, 32 (5W11): 81-88.

Kraus, K. 1993. *PHOTOGRAMMETRY*. Dümmler Verlag, Bonn., Vol.1, pp.277-279.

Kubik, K., 1991. Relative and absolute orientation based on linear features. *ISPRS Journal of Photogrammetry & Remote Sensing*, 46 (1): 199-204.

Mulawa, D. and Mikhail, E., 1988. Photogrammetric treatment of linear features. *Proceedings of International Archives of Photogrammetry and Remote Sensing*, Kyoto, Japan, Commission III, 27 (B10). 393 pages: 383-393.

Tommaselli, A. and Lugnani, J., 1988. An alternative mathematical model to collinearity equations using straight features. *Proceedings of International Archives of Photogrammetry and Remote Sensing*, Kyoto, Japan, Commission III, 27 (B3). 842 pages: 765-774.

Tommaselli, A. and Tozzi, C., 1992. A filtering-based approach to eye-in-hand robot vision. *Proceedings of International Archives of Photogrammetry and Remote Sensing*, Washington, USA, Commission V, 29 (B5). 950 pages: 182-189.

Tommaselli, A. and Poz, A., 1999. Line based orientation of aerial images. *Proceedings of the ISPRS Conference on Automatic Extraction of GIS Objects from Digital Imagery*, Munich, Germany, 32 (3-2W5). 226 pages: